



A cytosolic disulfide bridge-supported dimerization is crucial for stability and cellular distribution of Coxsackievirus B3 protein 3A

Martin Voss¹, Gunnar Kleinau², Niclas Gimber³, Katharina Janek¹, Clara Bredow¹, Fabien Thery^{4,5}, Francis Impens^{4,5,6}, Jan Schmoranzel³, Patrick Scheerer^{2,7} , Peter-Michael Kloetzel¹ and Antje Beling^{1,7} 

1 Charité – Universitätsmedizin Berlin, corporate member of Freie Universität Berlin and Humboldt-Universität zu Berlin, Institute of Biochemistry, Berlin, D-10117, Germany

2 Charité – Universitätsmedizin Berlin, corporate member of Freie Universität Berlin and Humboldt-Universität zu Berlin, Institute of Medical Physics and Biophysics, Group Protein X-ray Crystallography and Signal Transduction, Berlin, Germany

3 Charité – Universitätsmedizin Berlin, corporate member of Freie Universität Berlin and Humboldt-Universität zu Berlin, AMBIO - Advanced Medical Bioimaging Core Facility, Berlin, Germany

4 Department of Biomolecular Medicine, Ghent University, Belgium

5 VIB Center for Medical Biotechnology, Ghent, Belgium

6 VIB Proteomics Core, Ghent, Belgium

7 Deutsches Zentrum für Herz-Kreislauf-Forschung (DZHK), partner site Berlin, Germany

Keywords

coxsackievirus B3; enterovirus; homodimerization; infection; protein 3A

Correspondence

P.-M. Kloetzel and A. Beling, Charité – Universitätsmedizin Berlin, Institute of Biochemistry, Charitéplatz 1, 10117 Berlin, Germany

Tel: +49 30 450 528 071 (P-MK); +49 30 450 528 187 (AB)

E-mail: p-m.kloetzel@charite.de (P-MK); antje.beling@charite.de (AB)

(Received 5 October 2021, revised 20 December 2021, accepted 20 January 2022)

doi:10.1111/febs.16368

RNA viruses in the *Picornaviridae* family express a large 250 kDa viral polyprotein that is processed by virus-encoded proteinases into mature functional proteins with specific functions for virus replication. One of these proteins is the highly conserved enteroviral transmembrane protein 3A that assists in reorganizing cellular membranes associated with the Golgi apparatus. Here, we studied the molecular properties of the Coxsackievirus B3 (CVB3) protein 3A with regard to its dimerization and its functional stability. By applying mutational analysis and biochemical characterization, we demonstrate that protein 3A forms DTT-sensitive disulfide-linked dimers via a conserved cytosolic cysteine residue at position 38 (Cys38). Homodimerization of CVB3 protein 3A via Cys38 leads to profound stabilization of the protein, whereas a C38A mutation promotes a rapid proteasome-dependent elimination of its monomeric form. The lysosomotropic agent chloroquine (CQ) exerted only minor stabilizing effects on the 3A monomer but resulted in enrichment of the homodimer. Our experimental data demonstrate that disulfide linkages via a highly conserved Cys-residue in enteroviral protein 3A have an important role in the dimerization of this viral protein, thereby preserving its stability and functional integrity.

Abbreviations

ACBD3, acyl-CoA-Binding Domain-containing protein 3; CVA, coxsackievirus A; CVB, coxsackievirus B; EGFP, enhanced GFP; EM, epoxomicin; EV, Enterovirus; GOLD, GOLgi dynamic; HRV, Human RhinoVirus; KV, kobuvirus; LC3, microtubule-associated proteins 1A/1B Light Chain 3B; MOI, multiplicity of infection; NEM, N-ethylmaleimide; Nt, N-terminus; PDB ID, Protein Data Bank Identification Code; PV-1–3, poliovirus type 1–3; RCAS1, receptor binding cancer antigen expressed on SiSo cells 1; VP, viral protein; wt, wild-type.

Introduction

Enteroviruses (EVs) are implicated in an extensive range of clinical manifestations, such as pancreatitis, myocarditis and encephalitis [1,2]. They form an important genus within the large family of *Picornaviridae* and possess a positive-sense single-stranded 7.4 kb RNA genome, which encodes the viral polyprotein of 250 kDa. Viral 2A and 3C proteases cleave the viral polyprotein into intermediates and mature proteins to form the constituents necessary to assemble new virions [1]. The viral proteins include four capsid proteins (VP1–VP4), seven non-structural proteins (2A, 2B, 2C, 3A, 3B, 3C and 3D) as well as the functional precursor proteins (2BC, 3AB and 3CD). The viral protease 2A catalyzes the initial cleavage of the polyprotein and thereby releases the fragment P1 that contains the capsid proteins. Consequently, protease 3C and its stable precursor 3CD catalyze the cleavage of P1 and the processing of the fragments P2 (2A–C) and P3 (3A–D) [3].

We previously evidenced that infection with Coxsackievirus B3 (CVB3), a model pathogen of the EV genus, disturbs protein homeostasis at virus-utilized membranes and results in an accumulation of ubiquitinated proteins [4]. The enrichment of membrane-bound ubiquitin conjugates was shown to be attributed to the presence of the non-structural VPs 2B and 3A. Both proteins are known to be involved in the reorganization of cellular membranes and perturb membrane integrity. Mutations in protein 3A cause defects in viral replication [5] and it has been suggested, that protein 3A together with the Golgi adaptor protein acyl-CoA-binding domain-containing protein 3 (ACBD3) forms a scaffold for the generation of viral replication complexes and membrane remodeling [6,7]. Protein 3A is a small hydrophobic 87-residue protein consisting of a soluble N-terminus (Nt) and a hydrophobic C-terminus and is formed by the cleavage of the precursor protein 3AB into 3A and 3B. Yeast two-hybrid experiments revealed that full-length protein 3A has the ability to self-associate [7] and NMR spectroscopy studies demonstrated that protein 3A from poliovirus forms a symmetric homodimer via the soluble N-terminal domain, whereby its underlying molecular mechanism is not finally defined so far [5]. Corroborating these findings, we recently showed that CVB3 protein 3A can form SDS-resistant homodimers when expressed in HeLa cells [4]. This study was set up to investigate the molecular basis for the ability of the non-structural CVB3 protein 3A to form such SDS-resistant homodimers. We now show that protein 3A homodimerizes via a DTT-sensitive disulfide bridge between cysteine residues at position 38, thereby preserving its stability and

functional integrity. Because this cysteine is conserved among other enteroviral 3A proteins, our findings may have implications for other EVs.

Results

A disulfide bridge in the cytosol is crucial for the dimerization of CVB3 non-structural protein 3A

To investigate the molecular basis relevant for the formation of SDS resistant protein 3A homodimers, we used CVB3, an established model pathogen for enteroviral infection. HeLa cells were infected with CVB3 [multiplicity of infection (MOI) 0.1] for 16 h and the non-structural protein 3A was detected by immunoblotting. Analysis of CVB3-infected HeLa cells showed that, in addition to protein 3A and its precursor 3AB migrating at 10 and 12 kDa, respectively, a ladder of bands starting at 18 kDa was detected, with their intensity decreasing above 18 kDa (Fig. 1A). To test whether this band pattern represents some form of previously unknown post-translational modification of protein 3A or SDS-resistant interaction, N-terminally V5-tagged 3A (V5-3A) was expressed in HeLa cells. Indeed, identification of V5-3A by immunoblotting revealed, in addition to a primary band of V5-3A at 12 kDa, a prominent signal migrating at approximately 20 kDa (Fig. 1B). After having excluded that the observed band pattern was due to ubiquitylation, neddylation or conjugation with Urm1 we hypothesized that the 20 kDa signal may be indicative for the formation of dimer arrangements (data not shown).

To constrict the possible types of modification and residue(s) in CVB3 protein 3A responsible for the formation of the 20 kDa band, synthetic genes with particular amino acid substitutions were designed. Instead of mutating individual amino acid, multiple residues were mutated simultaneously, except for those located in the transmembrane domain (Fig. 1C). Initially, six constructs were generated carrying substitutions for all lysine residues (construct termed *c3A-K*), all serine residues (*c3A-S*), all threonine residues combined with tyrosine residues (*c3A-TY*), all arginine residues (*c3A-R*), all aspartic acid residues combined with asparagine residues (*c3A-DN*) and N-terminal cysteine 38 in conjunction with histidine 57 (*c3A-CH*). Of all mutations introduced into protein 3A, only the *c3A-CH* mutation led to an elimination of the observed band migrating at 20 kDa, indicating that either cysteine 38 or histidine 57 is required for generating the observed band shift on immunoblots (Fig. 1D). Therefore, we generated protein 3A variants with single substitutions of either cysteine 38 (*c3A-C*) or histidine 57 (*c3A-H*), respectively.

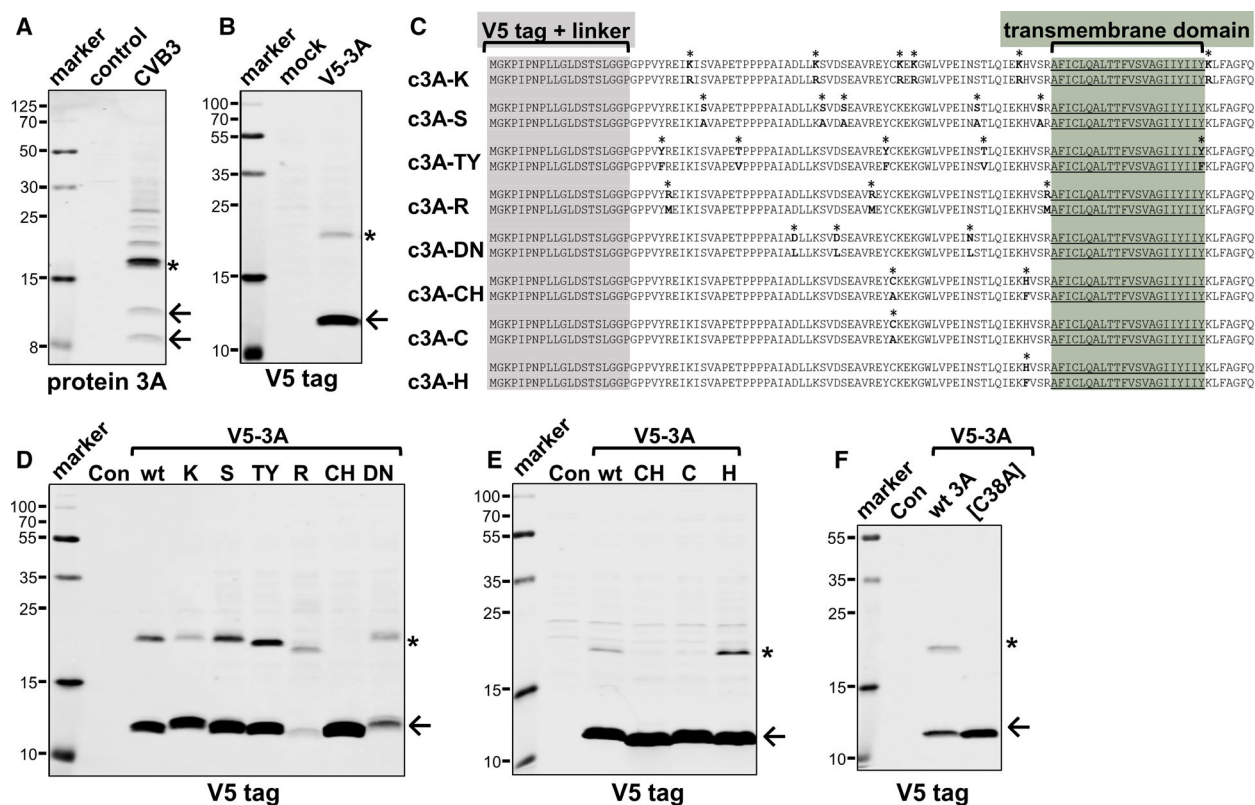


Fig. 1. Effect of amino acid substitutions on post-translational modification of CVB3 protein 3A. (A) HeLa cells treated $-/+$ CVB3 (MOI 0.1) for 16 h, were analyzed by immunoblotting of CVB3 protein 3A. Arrows indicate protein 3A (and 3AB) at the expected size, asterisks indicate signal with an increase of its apparent mass by 8 kDa. The lane designated as 'marker' contains prestained protein standards that are partially detectable by the Odyssey imaging system. (B) Immunoblotting of V5-tagged protein 3A (V5-3A) expressed in HeLa cells. (C) Synthetic genes of V5-tagged protein 3A, in which indicated types of amino acids were replaced by non-reactive amino acids, were cloned into a pcDNA3.1(+) expression vector. (D) Expression of wt V5-3A and variants in which all amino acids of the indicated type(s) were substituted. Non-transfected cells were used as negative control (Con). Protein extracts were prepared 48 h after transfection and analyzed by immunoblotting of V5 tag. (E) Expression of wt V5-3A and its CH variant with concurrent substitution of cysteine 38 and histidine 57 as well as variants with respective single substitutions. (F) Expression of wt and [C38A] variants of V5-3A.

Expression of both protein 3A variants demonstrated that the observed 8-kDa shift is based on a modification of the N-terminal cysteine 38 residue (Fig. 1E), located in the cytosolic domain (Fig. 1C). The expression of a V5-3A C38A variant further confirmed the essential role of Cys38 in the CVB3 for establishing the 20 kDa CVB3 protein 3A form (Fig. 1F).

Even though cysteine 38 (C38) of CVB3 protein 3A is located in its cytosolic domain, we hypothesized that the observed shift in molecular weight is indicative of a disulfide-linked homodimer. Therefore, wildtype (wt) 3A and a C38A variant (3A [C38A]) were cloned into pEGFP-C3 for expression in HeLa cells. Immunoblotting revealed the expected protein band at 40 kDa for both 3A variants (Fig. 2A). However, in the case of wt protein 3A, an additional DTT sensitive band occurred at 82 kDa, supporting our hypothesis that protein 3A forms a disulfide-linked homodimer (Fig. 2A). This

finding was corroborated by the expression of 6xHis-V5-3A in *Escherichia coli* BL21 cells. The analysis of a Ni-NTA-based pull-down assay did not only show enrichment of monomeric 6xHis-V5-3A at 15 kDa but also of the dimeric form migrating at 32 kDa (Fig. 2B). Liquid chromatography–mass spectrometry (LC–MS)/MS analysis of protein bands at 15 and 32 kDa confirmed that both species represent protein 3A (Fig. 2C).

The fact that the higher molecular weight protein 3A complex was maintained in the presence of urea (Fig. 2D) revealed that its formation was not due to artificial hydrogen bond formation during SDS gel electrophoresis. To also exclude the possibility that protein 3A forms stable disulfide bonds after cell lysis, protein samples were prepared with and without the thiol-reactive alkylating agent *N*-ethylmaleimide (NEM) to block free accessible cysteine residues. NEM also inactivates cysteine proteases, for example,

ubiquitin peptidases, as well as cellular mechanisms that reduce disulfide bonds, for example, glutathione and protein disulfide isomerases. In the presence of

NEM during lysis, the modified form of protein 3A was maintained and occurred even at higher levels compared to lysis buffer without the alkylating agent,

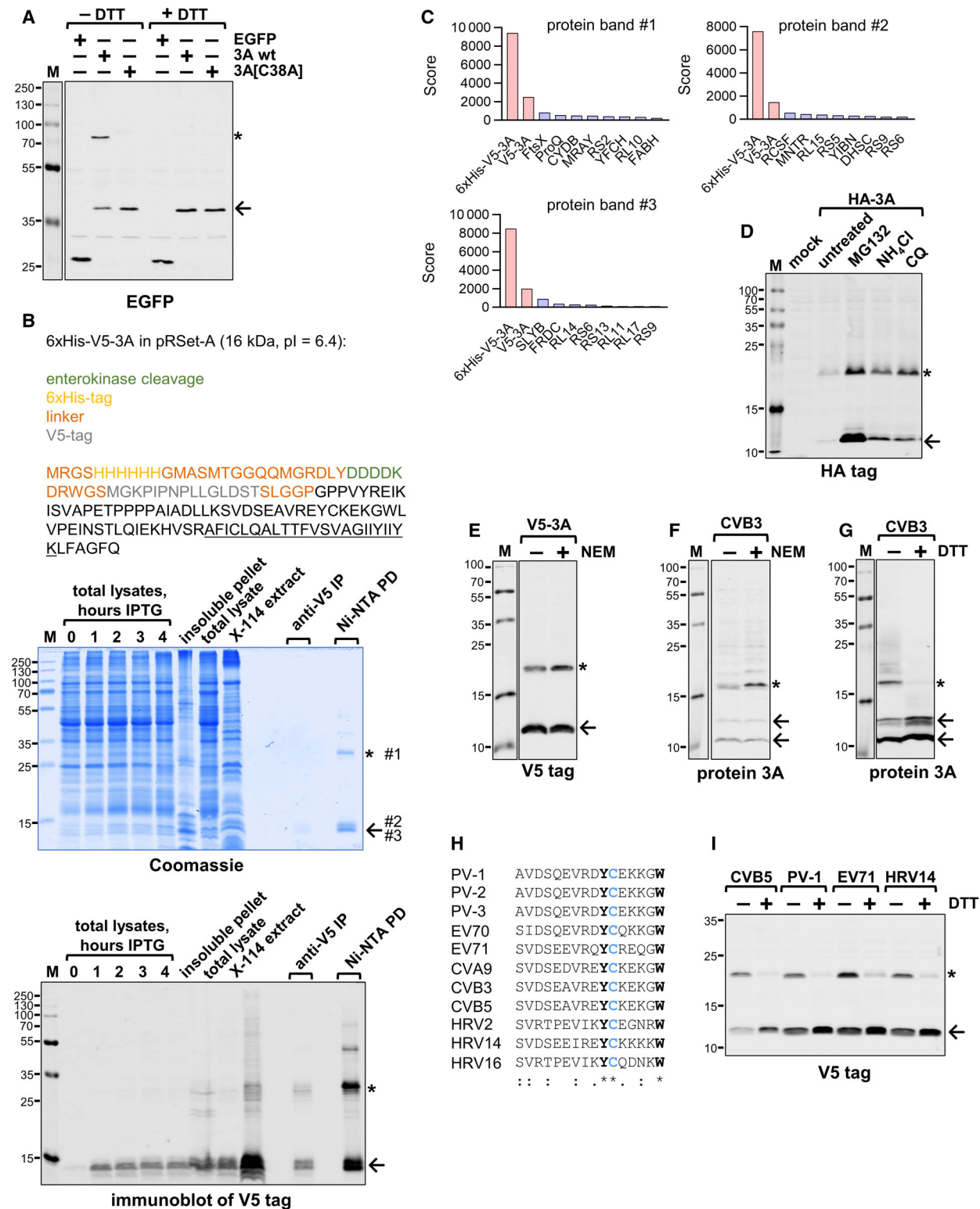


Fig. 2. Cysteine-dependent dimerization of CVB3 protein 3A. (A) EGFP-tagged protein 3A and 3A[C38A] expressed in HeLa cells were analyzed by immunoblotting of GFP in samples prepared $-/+$ DTT. The arrow indicates EGFP-3A at 40 kDa, while the asterisk indicates the dimer at 82 kDa. The lane designated as 'M' (marker) contains prestained protein standards. (B) Bacterial expression of CVB3 protein 3A. The sequence of 6xHis-V5-3A cloned into pRSet-A and expressed in *Escherichia coli* BL21 cells. IPTG was added at a final concentration of 0.5 mM when the culture reached an OD of 0.7 and cells were collected at indicated points in time in lysis buffer supplemented with Triton X-114. Total lysates of all points in time and the Triton-insoluble pellet, as well as a Triton X-114 extract (10-fold concentrated) of 4 h IPTG, were prepared for SDS/PAGE. Aliquots of the Triton X-114 phase of cell extracts were diluted in lysis buffer supplemented with 0.5% CHAPS and incubated at 4 °C with magnetic Ni-NTA resin for pulldown (PD) or anti-V5 agarose for immunoprecipitation (IP) of 6xHis-V5-3A. Bound proteins were eluted with SDS/PAGE sample buffer and heated at 95 °C for 5 min. All samples were analyzed by Coomassie staining (middle panel) and immunoblotting of the V5 tag (lower panel). Indicated protein bands of the Coomassie-stained SDS PAGE (middle panel) marked by the asterisk (protein band #1) and the arrow (upper protein band #2, lower protein band #3) were excised and analyzed by mass spectrometry. (C) Sum of highest ion scores as determined by LC-MS/MS for the 10 most abundant proteins within the respective protein bands shown in the Coomassie-stained SDS PAGE in (B). 6xHis-V5-3A and V5-3A are colored in red, *Escherichia coli* proteins in blue. (D) Cells transfected with an empty vector (mock) were used as control. Cells were treated with 5 μ M MG132, 25 mM NH₄Cl or 125 μ M CQ for 16 h, and then lysed in lysis buffer supplemented with 8 M urea. Protein samples prepared in Laemmli buffer supplemented with 6 M urea, separated on a 15% Tris-glycine-urea containing 6 M urea, and analyzed by immunoblotting of HA tag. (E) V5-3A transfected and (F) CVB3 infected HeLa cells (MOI 0.1, 16 h) were processed in lysis buffer $-/+$ NEM and analyzed by immunoblotting of V5 tag and CVB3 protein 3A, respectively. Arrows indicate protein 3A (and upper band protein 3AB) at the expected size, asterisks indicate homodimer. (G) HeLa cells were infected with CVB3 (MOI 0.1) for 16 h. Protein samples were incubated at 95 °C for 5 min $-/+$ 100 mM DTT. Arrows indicate protein 3A (and upper band protein 3AB) at the expected size, asterisks indicate signal with an increase of its apparent mass by 8 kDa. (H) Multiple sequence alignment of protein 3A of representatives of the EV genus (CVA: coxsackievirus A). (I) Immunoblotting of V5-3A of CVB3, PV-1, EV71 and HRV14. (J) HA-tagged protein 3A encoding cDNA was transfected into HeLa cells.

demonstrating that disulfide bridging via cysteine 38 is already formed within the cell (Fig. 2E,F). In all subsequent experiments, the lysis buffer was therefore supplemented with NEM to maintain the disulfide-linked complex and to avoid artificial disulfide linkages. Nevertheless, the levels of modified V5-3A showed a certain degree of variation with an average ratio of monomer to dimer of 4 ± 1 after expression for 24 h.

A protein 3A sequence comparison of representatives of the EV genus revealed that the cysteine residue at position 38 of CVB3 protein 3A is highly conserved, suggesting that cysteine-dependent dimerization might occur also in related species. In support, expression of protein 3A from CVB5, poliovirus type 1 (PV-1), EV 71 and rhinovirus 14, showed the same pattern of DTT-sensitive modification as demonstrated for CVB3 (Fig. 2G–I). In summary, these data suggest that cysteine-linked dimerization is a common feature of enteroviral protein 3A.

An alternative disulfide bridge at the predicted protein 3A dimer interface rescues C38A induced dimer separation

The structure of a homodimer of enteroviral protein 3A was previously determined and its role in CVB3 replication characterized, but the residues identified to maintain dimerization did not include cysteine 38 [5]. We here designed a structural homology model of the CVB3 3A protein based on the kobuvirus (KV)

protein 3A in complex to the ACBD3 GOLgi dynamic (GOLD) domain [Protein Data Bank (PDB) ID: 6q69] [8]. The model was designed to simulate the experimentally verified assembly of a disulfide-linked CVB3 protein 3A homodimer (Fig. 3A,B), to unravel structural consequences and proof on the reliability of experimental observations. First, the disulfide-linked CVB3 protein 3A homodimer proposed here differs slightly in inter-helical arrangement compared to known protein 3A structures (PDB IDs: 6q69 [8] and 1ng7 [9]) without a covalently linked disulfide bridge, while the intrahelical interaction of the individual protomers is similar (Fig. 3C). However, in our structural model, several intermolecular interactions such as K41/D24 are observed between the two linked protomers, as well as between K41/D25 or V34/V34, which were also identified in the already known crystal structure of the N-terminal domain of protein 3A (Fig. 3D). Second, to confirm the model-based prediction of interaction sites between two 3A monomers and the importance of a disulfide bridge, a new protein 3A variant C38A/V34C was designed. According to our structural model, positions 34 of both protomers are at an ideal spatial distance from each other (Fig. 3D) to form a new disulfide bridge by substituting V34C, as an alternative to the disrupted disulfide bridge by the C38A variant. Indeed, based on this model prediction, a new disulfide bridge was formed between the two protein 3A monomers in the C38A variant, which was confirmed by a rescue of protein 3A dimerization (Fig. 3E).

Dimerization of protein 3A influences its route of degradation and cellular distribution

Having established that CVB3 protein 3A forms a homodimer via a cytosolic disulfide bridge, we investigated the effect of homodimerization on protein stability in cycloheximide chase experiments. Homodimerization of protein

3A resulted in a significant stabilization of the protein (Fig. 4A), whereas the monomeric form of V5-tagged 3A was rapidly degraded and exhibited a half-life of ~ 6 h (Fig. 4A). To clarify the rapid turnover of monomeric protein 3A, inhibitory effects on protein degradation pathways were examined (Fig. 4B). Treatment of transfected

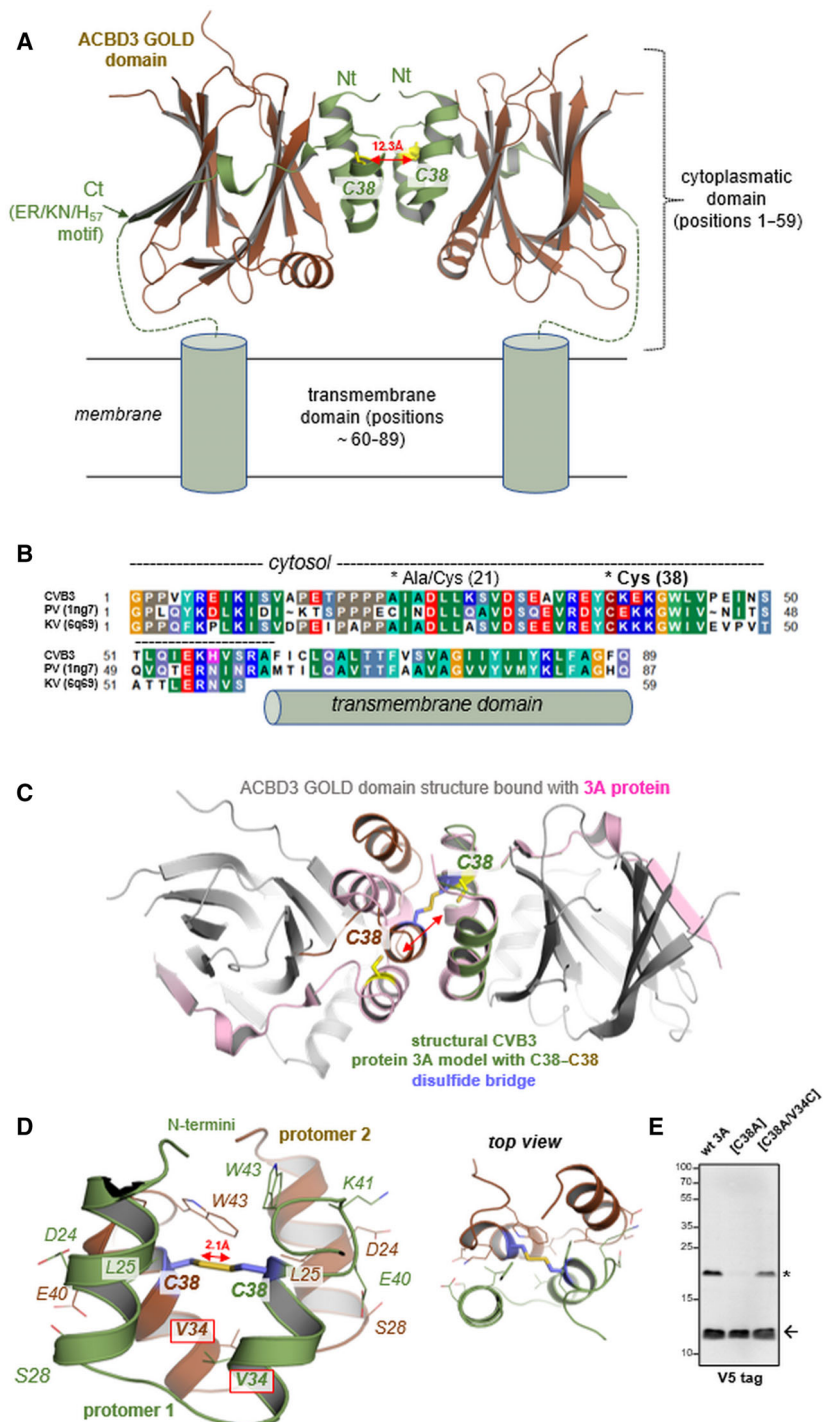


Fig. 3. *In silico* model of a putative CVB3 protein 3A homodimer linked via a disulfide bridge between cysteines at position 38. (A) Principle structure of protein 3A. This figure shows structural features (backbone cartoon) of protein 3A (green) bound with the ACBD3 GOLD domain (brown) as known from a crystal structure of EV-G1 (PDB ID: 6q69 [8]). The combination with schematic transmembrane domains (cylinder) visualizes the principle arrangement of the non-covalently linked complex. (B) Sequence comparison between 3A proteins of CVB3, poliovirus (PV) and KV. The numbers after abbreviations indicate respective protein database [11] ID's of already determined PV and KV protein 3A structures. The alignment (Blossum62 matrix) was visualized using the software BioEdit Hall TA (BioEdit: a user-friendly biological sequence alignment editor and analysis program for Windows 95/98/NT). Nucleic Acids Symposium Series 41, 95-98 (1999). Specific background colors indicate the type of amino acid, conservation and distinct chemical properties of amino acid side chains: black-proline; blue-positively charged; red-negatively charged; cyan/green-aromatic and hydrophobic; green-hydrophobic; gray-hydrophilic; dark red-cysteines and magenta-histidine. (C) The ACBD3 GOLD domain structure (gray cartoon backbone) bound with KV protein 3A (light-magenta) was previously determined (PDB ID: 6q69 [8]) and served here as a template for structural homology modeling of the CVB3 protein 3A disulfide-linked homodimer (green). Superimposition between the KV 3A protein structure and the CVB3 3A protein model illustrates changes in interhelical arrangements of dimer-formation due to a structural constraint by the experimentally evidenced disulfide bridge. (D) Detailed view on the protein A dimer interface, whereby the protomers 1 and 2 are connected by a disulfide bridge. Several amino acids (lines) of both protomers are in close distance to each other, for example, as V34 or W43. (E) Disulfide rescue of protein 3A [C38A] dimerization by substitution of valine 34 with cysteine (3A [C38A/V34C]). V5-tagged protein 3A variants with indicated amino acid substitutions were transfected into HeLa cells. Forty-eight hours after transfection, protein lysates were analyzed by immunoblotting of the V5 tag. The position of V34 is depicted in the homology model of a disulfide-linked protein 3A homodimer (D).

cells with the proteasome inhibitor epoxomicin (EM) resulted in a ~40-fold increase of monomeric non-modified V5-3A. Proteasome inhibition also led to 13-fold enrichment of the homodimer, which is most likely indirectly due to EM-dependent accumulation of monomers as a prerequisite for dimerization. Accordingly, the lysosomotropic agent CQ had only a minor effect on monomeric V5-3A but caused an approximately 30-fold enrichment of the homodimer (Fig. 4B).

The monomer formed by mutant V5-3A[C38A] exhibited a similar short half-life as monomeric wt V5-3A (Fig. 4C) and was also strongly stabilized in response to EM (Fig. 4D). Treatment with CQ resulted in a 7.5-fold enrichment of monomeric V5-3A[C38A], indicating that a minor fraction of protein 3A is diverted to lysosomal degradation as a monomer or non-covalent dimer as well. Taken together, these results demonstrate that monomeric protein 3A is primarily degraded by the proteasome, while as a homodimer it is shunted to the autophagy/lysosomal pathway.

To elucidate the involvement of autophagic pathways in the degradation of disulfide-linked protein 3A, we investigated the autophagy marker microtubule-associated proteins 1A/1B Light Chain 3B (LC3). Immunoblotting showed that the levels of lipidated LC3, an indication for autophagosome formation, were significantly higher during expression of wt V5-3A compared to V5-3A[C38A] (Fig. 4F). In comparison to mock-transfected control cells, a slight, although a not significant increase in lipidated LC3 occurred also in V5-3A[C38A] transfected cells, supporting the results of the CQ experiment indicating that a minor fraction of protein 3A as a monomer or non-covalent dimer is degraded via autophagic pathways. Correspondingly, studying the LC3 expression

by immunofluorescence in optical sections acquired by confocal microscopy showed that in cells transfected with enhanced GFP-tagged V5-3A (EGFP-V5-3A) variants forming disulfide-linked homodimers, the number of LC3-positive puncta indicative of autophagosomes was significantly increased (Fig. 5A).

Furthermore, confocal microscopy also revealed that wt protein 3A and 3A[C38A] exhibit differences regarding their cellular distribution. Whereas EGFP-V5-3A is concentrated at numerous small structures displaying a high intensity of the EGFP fluorescence signal, EGFP-V5-3A[C38A] was predominantly localized near the nucleus complemented by faint staining throughout the cell (Fig. 5A,B). Co-staining of the Golgi marker receptor binding cancer antigen expressed on SiSo cells 1 (RCAS1) showed that both 3A variants co-localize with membranes of the Golgi apparatus (Fig. 5B). However, in the case of wt protein 3A, the cellular distribution during its prolonged-expression entails a disruption of the Golgi complex, supporting a previous observation [9]. A quantitative comparison of EGFP-V5-3A fluorescence intensities showed a significant difference in intensity distribution between wt protein 3A and 3A[C38A] with a higher likelihood of bright pixels in the wt condition (Fig. 5C). In addition, the EGFP-V5-3A fluorescence was analyzed by autocorrelation-based image correlation spectroscopy, revealing bigger cluster sizes of staining clusters in the case of 3A[C38A] due to its widespread distribution (Fig. 5D). This analysis confirmed the different distribution pattern of wt and mutated protein 3A and together with the biochemical analysis demonstrates that cysteine-dependent dimerization of protein 3A directs its subcellular localization towards highly condensed membrane structures occupied by protein 3A.

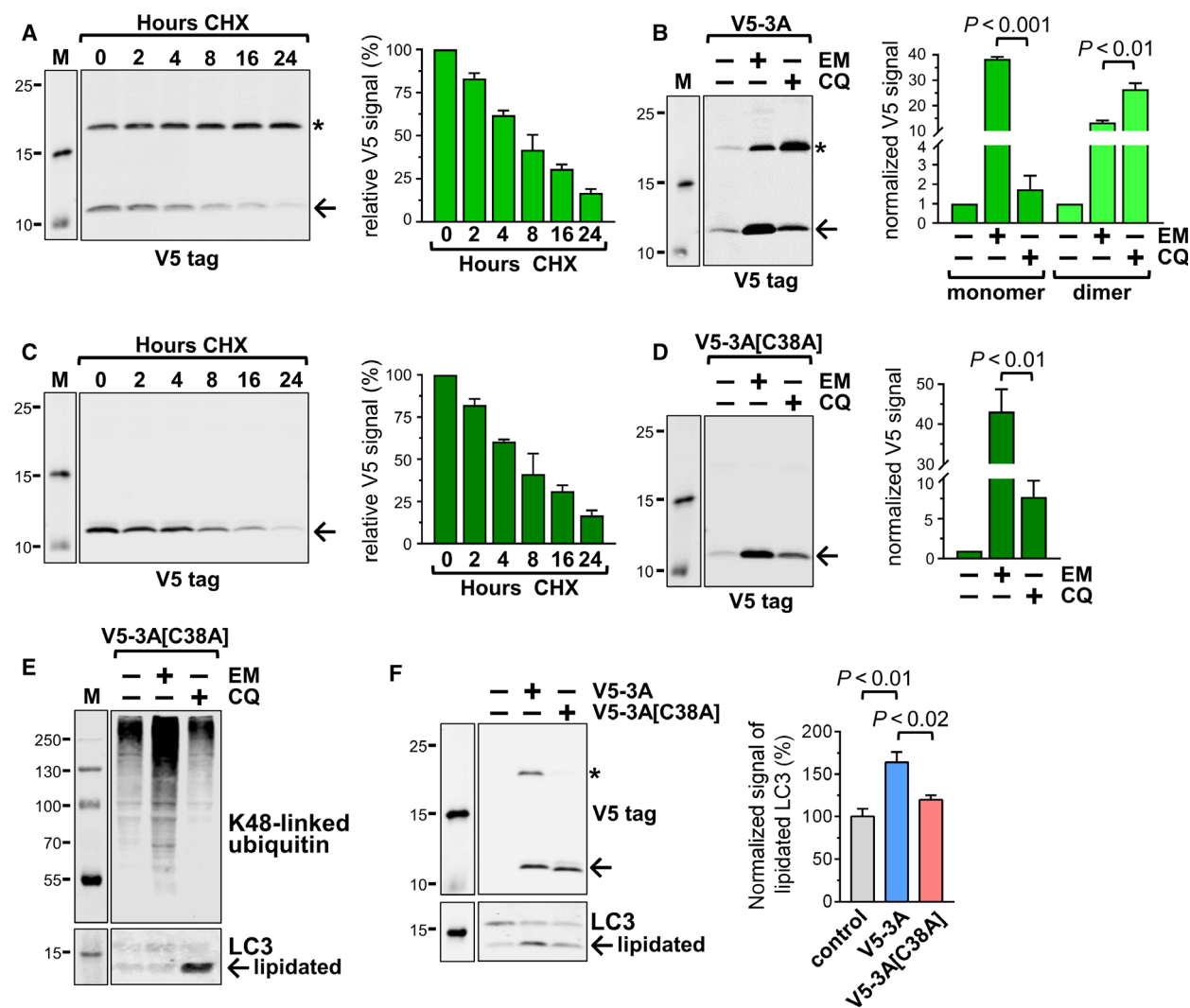
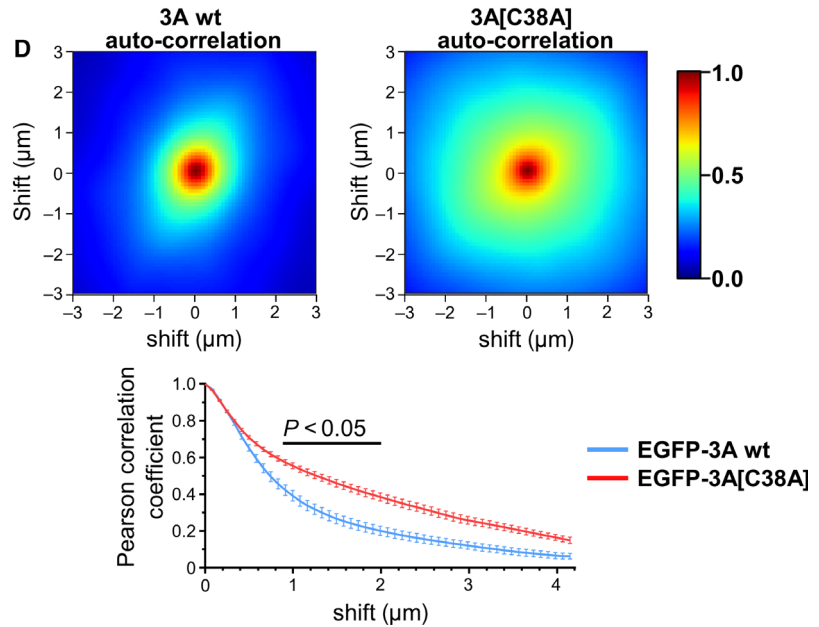
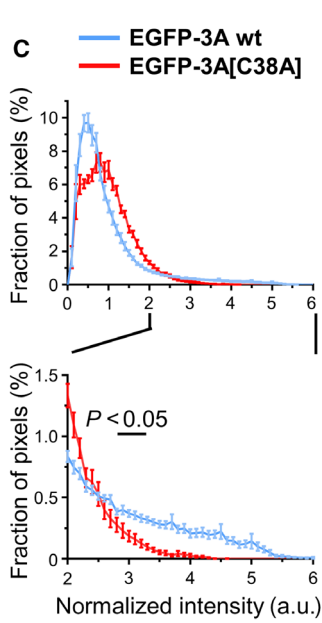
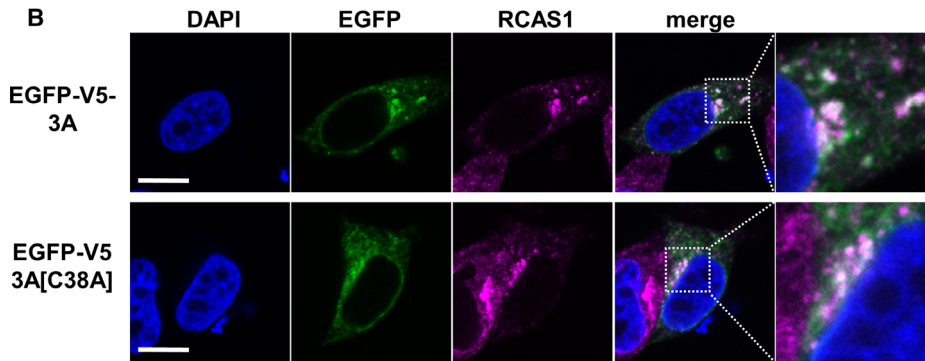
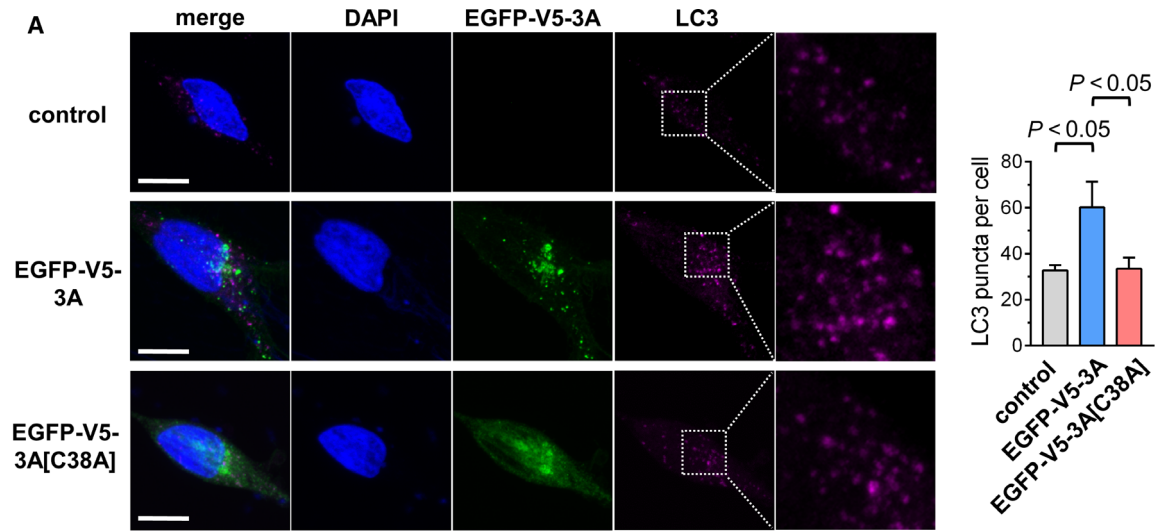


Fig. 4. Dimerization of protein 3A determines its route of degradation. (A) V5-3A transfected cells were collected at the indicated points in time after the start of treatment with cycloheximide (CHX) and processed for immunoblotting of V5 tag. The signal of the monomer at 12 kDa was quantified ($n = 4$). The lane designated as 'M' (marker) contains prestained protein standards. (B) Ten hours after transfection with V5-3A, cells were treated with EM or CQ for 14 h and analyzed by immunoblotting. Signals of V5-3A detected at 12 and 20 kDa were quantified ($n = 3$). (C) V5-3A[C38A] transfected cells were collected at the indicated points in time after the start of treatment with cycloheximide (CHX) and processed for immunoblotting of the V5 tag. The signal at 12 kDa was quantified ($n = 2$). (D) Ten hours after transfection with V5-3A[C38A], cells were treated with EM or CQ for 14 h and analyzed by immunoblotting. Signals of V5-3A detected at 12 kDa were quantified ($n = 3$). (E) K48-linked ubiquitin and LC3 were immunoblotted as controls to verify the efficacy of the applied inhibitors. (F) Immunoblotting of LC3 in HeLa cells transfected with empty vector (mock) or V5-3A variants for 24 h. The signal of lipidated LC3 was quantified ($n = 4$).

Fig. 5. Cysteine-dependent dimerization of CVB3 protein 3A directs its subcellular distribution. (A) Maximum intensity Z-projection of optical sections of cells transfected with EGFP-V5 tagged variants of protein 3A. Staining of DAPI (blue), EGFP-V5-3A (green) and LC3 (magenta). Scale bar: 10 μm . The bar chart summarizes the average number of LC3-positive puncta per cell in optical sections ($n = 12$). (B) Confocal microscopy of cells transfected with EGFP-V5 tagged variants of protein 3A for 24 h. Staining of DNA (DAPI, blue) and Golgi resident protein RCAS1 (magenta). Scale bar: 10 μm . (C) Quantitative comparison of EGFP fluorescence intensity distributions ($n = 15$) depicted in (B). (D) Autocorrelation-based image correlation spectroscopy of EGFP fluorescence shown in (B). 2D-plots depicting auto-correlation of x/y shifted confocal images to assess cluster sizes, which are collapsed into a 1D-Pearson correlation coefficient plot ($n = 15$).



Discussion

The CVB3 3A protein, which is associated with membranes via its hydrophobic C-terminal domain (Fig. 3), is involved in multiple steps of viral replication and, as such, an important interaction partner of the ACBD3 [6], forming a high molecular weight protein 3A-ACBD3 hetero-tetramer complex [7]. In this study, we show that the CVB3 3A protein on the cytosolic leaflet of cellular membranes can form a disulfide bridge via residue C38, resulting in an SDS-resistant stabilization of the protein 3A homodimer, and that this is a conserved feature of EVs.

NMR studies previously showed that the 3A protein can form a non-covalent homodimer (PDB ID: 1ng7) [10]. In addition, protein X-ray crystallography (PDB ID: 6q69 [8]) identified residues L25, V34, Y37 forming the hydrophobic core of the protein 3A dimerization interface that is flanked by a salt bridge. This salt bridge is formed by the residues K41 and D24 when associated with the ACBD3 GOLD domain [7]. However, the existence of disulfide bridges formed by the conserved C38 residue of protein 3A was not indicated in either study. This difference may be explained by the fact that the crystallographic studies were performed under reducing conditions in the presence of β -mercaptoethanol or tris(2-carboxyethyl)phosphine, which result in a selective irreversible reduction of disulfide bridges in cysteine-containing proteins. Also, the CVB3 3A protein can crystallize as a monomer as well as a dimer, suggesting that in the absence of cysteine bridges hydrophobic packaging as outlined above stabilizes the crystal. Interestingly, modelling of covalent protein 3A homodimers and comparison with published protein 3A structures (PDB IDs: 6q69 [8] and 1ng7 [9]), lacking the C38 disulfide bridge, indicates that the introduction of a covalently linked disulfide bridge causes minor structural changes that affect several intermolecular interactions between the protomers.

Besides co-localization with the Golgi network, our immunofluorescence studies of ectopically expressed 3A proteins also show the introduction of a C38A mutation into the 3A protein and thus the inability to homodimerize via C38 disulfide bridges does not have any profound effect on its ability to interact with membranes. Nevertheless, slight differences between wt 3A and 3A[C38A] protein do exist with regard to their intracellular distribution, whereby the ability to form homodimers via disulfide bridges leads to an enhanced decoration of more highly condensed protein 3A-occupied membrane structures. In accordance with our biochemical data, this more localized accumulation of

wt 3A close to the Golgi apparatus may be due to the observed increased stability of 3A homodimers.

The formation of disulfide bridges in the cytosol is strongly dependent on the redox state in a specific cellular compartment. In this context, we have previously shown that in particular membrane proteins are susceptible to oxidative damage, indicating that protein 3A being a transmembrane protein is indeed exposed to a cellular redox milieu that can promote the formation of a disulfide linkage and homodimer formation [4]. Multimeric protein complexes are known to be more resistant to damage by reactive oxygen species. Our data indeed demonstrate that the C38 linked disulfide bridge and protein 3A homodimer formation results in a significant stabilization of protein 3A, thereby increasing cellular 3A homodimer levels.

As shown by Horova and coworkers [7], homodimeric 3A forms an essential membrane-bound platform for the formation of hetero-tetrameric 3A/ACBD3 complexes and hence the recruitment of other proteins that are pivotal for effective virus replication. Stabilization of protein 3A by disulfide-bridges may therefore be a means to prevent proteasomal degradation during the early phase of infection as well as to provide sufficient protein for the formation of the replication platform.

Materials and Methods

Cell culture

HeLa cells (ATCC, Manassas, VA, USA) were maintained in Dulbecco's Modified Eagle Medium supplemented with 10% (v/v) FBS and 1% (v/v) penicillin/streptomycin (all reagents from Thermo Scientific, Seattle, MA, USA). For transient transfections, cells were grown to 90% confluence and transfected with 0.5 μ g expression vector per 1×10^5 cells using Polyethylenimine – Linear, MW 25000 (Polyscience, Inc, Hirschberg, Germany). Medium was replaced 8 h after transfection. Where indicated, cells were treated with 50 μ g·mL⁻¹ cycloheximide, 180 nM EM or 100 μ M CQ (all compounds from Sigma–Aldrich, Saint Louis, MO, USA).

Expression constructs

The V5 tag is a short peptide tag for the detection and purification of proteins and this was cloned at the Nt of the 3A protein. Synthetic genes of V5-tagged CVB3 (strain Nancy) protein 3A and its variants were synthesized by Integrated DNA Technologies (Coralville, IA, USA) and cloned into a pcDNA3.1(+) (Thermo Scientific) or pEGFP-C3 (Clontech, Mountain View, CA, USA) expression vector. For protein expression in *E. coli*, V5 tagged protein 3A was cloned into pRSet-A-6-His (Thermo Scientific).

Bacterial expression

Recombinant plasmid pRSet-A encoding 6xHis-V5 tagged protein 3A was transformed into *E. coli* BL21 (New England Bio-Labs GmbH, Frankfurt am Main, Germany) by heat shock. Recovered cells were plated on LB agar with 100 $\mu\text{g}\cdot\text{mL}^{-1}$ ampicillin and incubated at 37 °C overnight. A single colony was used to inoculate 10 mL of LB medium supplemented with ampicillin and incubated at 37 °C overnight with shaking. The starter culture was diluted to 200 mL with antibiotic-free LB medium and incubated at 37 °C with shaking. IPTG (Thermo Scientific) was added at a final concentration of 0.5 mM when the culture reached an OD of 0.7, and cells were collected at the required points in time by centrifugation at 4600 g for 20 min.

Cell lysis and Triton X-114 extraction

Adherent cultures of HeLa cells were scraped off, pelleted by centrifugation at 2000 g for 3 min, washed in PBS, pelleted again and the cell pellet lysed in 20 mM Hepes pH 7.4, 1% (v/v) Triton X-114, 8 mM EDTA, 2 mM EGTA, Complete protease inhibitor (Roche, Basel, Switzerland), 50 mM NaF, 5 mM Na-pyrophosphate, 2 mM Na-o-vanadate and 10 mM NEM. After incubation on ice for 20 min, lysates were centrifuged at 16 000 g (4 °C) for 10 min to pellet debris. Protein concentration was determined by the Bradford assay. For extraction of membrane proteins by phase separation of Triton X-114 (Sigma–Aldrich), cleared lysate was incubated at 25 °C for 5 min, centrifuged at room temperature at 5000 g for 5 min and the upper aqueous phase aspirated. The detergent phase was resuspended in ice-cold PBS and subjected again to phase separation. The obtained detergent phase was used for downstream applications.

Pull-down experiments

For a 6xHis pull-down of 6xHis-V5-3A expressed in *E. coli* BL21, cells were lysed in 100 mM Tris pH 8.0, 1% (v/v) Triton X-114, 4 mM EDTA, 1 mM EGTA, Complete protease inhibitor, 100 mM NaCl. The Triton X-114 phase of cell extracts was diluted in lysis buffer supplemented with 0.5% CHAPS and incubated at 4 °C with magnetic Ni-NTA resin (Thermo Scientific) for 60 min. The resin was washed three times with lysis buffer supplemented with CHAPS. Bound proteins were eluted with SDS/PAGE sample buffer and heated at 95 °C for 5 min.

Immunoblotting

SDS/PAGE was performed on 12%, 15%, or 4–15% (Bio-Rad Laboratories GmbH, Feldkirchen, Germany) Tris-glycine gels using Tris-glycine running buffer. For SDS/PAGE, protein samples were prepared in 62.5 mM Tris HCl pH 6.8, 10% Glycerol, 2% SDS, 0.005% Bromophenol Blue. The transfer of proteins onto 0.2- μm nitrocellulose membrane

(Licor Bioscience, Lincoln, NE, USA) was carried out using Towbin buffer for tank blotting or discontinuous Tris-CAPS buffer for semi-dry blotting (Bio-Rad Laboratories GmbH, Feldkirchen, Germany). Immunostaining was performed according to standard protocols. The following primary antibodies were used: V5 (Thermo Scientific), GFP (Thermo Scientific), GAPDH (Thermo Scientific & Abcam, Cambridge, UK), LC3-A/B (Cell Signaling, Danvers, MA, USA), and p62 (Enzo, Farmingdale, NY, USA). Anti-3A antibody was a gift from J. L. Whitton (The Scripps Research Institute, USA). Secondary IRD680CW or IRDye800CW labeled antibodies (Li-Cor Biosciences, Lincoln, NE, USA) were visualized using an Odyssey CLx imager and analyzed with Image Studio software (Li-Cor Biosciences).

Modeling of a coxsackievirus B3 protein 3A homodimeric structure linked via a disulfide bridge

Reasoned by high sequence similarity of > 70% the KV protein 3A (PDB ID: 6q69) domain bound with the Acyl-CoA-binding domain-containing protein-3 GOLD served as a template for homology modeling of the CVB3 protein 3A homodimer. In brief, the template ACBD3 domain was deleted and the remaining KV protein 3A structure sequence was substituted *in silico* by the sequence of the CVB3 3A protein according to the sequence alignment (Fig. 3B). For modeling procedures, the SYBYL X2.0 software (Certara, NJ, USA) was used. This preliminary model was energetically refined by AMBER F99 force field energy minimization until converging at a termination gradient of 0.05 kcal/mol*Å. Based on the experimental findings supporting a disulfide-linked CVB3 protein 3A homodimer (functional constraint), one protomer was manually shifted relative to the second protomer in a spatial distance that enables a disulfide bridge. A disulfide bridge between both cysteines at position 38 was created. By constraining one of the two interrelated CVB3 protein 3A protomer backbones, the distances between both protomers and interacting side chains were optimized via energy minimization, followed by a short dynamic simulation (1 ns) of side chains. The resulting dimeric interface was energetically minimized.

Immunofluorescence

For immunofluorescence microscopy cells were seeded on 13-mm coverslips coated with poly-lysine (Sigma–Aldrich). For anti-3A (provided by K. Klingel, University of Tübingen, Germany) and anti-RCAS1 (Cell Signaling) immunofluorescence, cells were fixed with 4% paraformaldehyde in PBS for 20 min and then rinsed with PBS. After permeabilization with 0.2% Triton X-100 for 10 min, non-specific binding sites were blocked with 4% FBS in PBS supplemented with 0.1% Triton X-100 for 30 min. Incubation with primary antibody was performed in blocking

solution at room temperature for 2 h. After three washing steps with PBS, samples were incubated with Alexa Fluor 568 coupled secondary antibody (Thermo Scientific) in blocking solution for 1 h. After three washing steps with PBS and a rinse in ultra-pure water, samples were mounted on microscope slides using ROTI-Mount Fluoro-Care DAPI (Carl Roth, Karlsruhe, Germany). Images were acquired on a Nikon Scanning Confocal A1Rsi+ (Nikon Europe BV, Amsterdam, the Netherlands) using a Plan Fluor 63x Oil objective (NA = 1.3).

For the quantitative comparison of immunofluorescence intensity distributions, confocal images in an 8-bit grayscale were analyzed using IMAGEJ [12]. The area of a cell excluding the nucleus was defined as the region of interest to determine the intensity distribution of anti-3A immunofluorescence. The intensities of the anti-3A staining in the region of interest were normalized to its mean intensity and intensity distributions were represented as the percentage of pixels of a particular normalized intensity.

For anti-LC3B (Cell Signaling) immunofluorescence, cells were fixed with 100% cold methanol for 20 min at –20 °C and then rinsed with PBS. Non-specific binding sites were blocked with 4% FBS in PBS supplemented with 0.1% Triton X-100 for 30 min. Incubation with primary antibody was performed in blocking solution at room temperature for 2 h. After three washing steps with PBS, samples were incubated with Alexa Fluor 568 coupled secondary antibody in blocking solution for 1 h. In methanol-fixed samples, EGFP-V5-3A was stained using an anti V5 antibody and Alexa Fluor 488 coupled secondary antibody (Thermo Scientific). After three washing steps with PBS and a rinse in ultra-pure water, samples were mounted on microscope slides using ROTI-Mount Fluoro-Care DAPI. Images were acquired on a Nikon Scanning Confocal A1Rsi+ using a Plan Fluor 63x Oil objective (NA = 1.3). Optical sections were acquired in accordance with the Nyquist theorem. Anti-LC3 puncta in optical sections were determined using the 3D objects counter plugin for Fiji (IMAGEJ).

Autocorrelation-based ICS of anti-3A immunofluorescence

Autocorrelation-based image correlation spectroscopy (ICS) was applied to confocal images to compare cluster sizes. Regions with protein 3A signal were automatically selected by Otsu's method. Images were then autocorrelated after shifting them pixel-wise against themselves along the *x*- and *y*-axes. Pearson coefficients were calculated for each shift and plotted against the shift. In this analysis, large and small structures can be readily distinguished by their broad or narrow distribution of autocorrelation values, respectively. The custom written python script is available as a Jupyter Notebook: <https://github.com/ngimber/ImageCorrelationSpectroscopy>

Multiple sequence alignment

Sequences of protein 3A from representatives of the EV genus were obtained from the UniProt knowledgebase under accession number P03300 (PV1), P06210 (PV2), P03302 (PV3), P32537 (human EV 71), Q66478 (human EV 71), P04936 (human rhinovirus 2, HRV2), Q82122 (HRV 16), P03303 (HRV 14), P21404 (coxsackievirus A9), P03313 (CVB3) and A0A2P1C6L8 (CVB5). The multiple sequence alignment was performed using ClustalW with a Blosum matrix on the ExpPASy bioinformatics resource portal.

Protein identification after in-gel digestion and LC-MS/MS analysis

Samples of enriched protein 3A were separated on a 15% SDS gel. Excised protein bands corresponding to the apparent molecular mass of 3A homo-dimer were subjected to in-gel digestion with trypsin. LC-MS/MS analysis of peptides was performed on an Ultimate 3000 RSLCnano system online coupled to an Orbitrap Q Excative Plus mass spectrometer (Thermo Scientific). The system comprised a 75 μ m i.d. \times 250 mm nano LC column (Acclaim PepMap C18, 2 μ m; 100 Å; Thermo Scientific). Full MS spectra (350–1600 *m/z*) were acquired at a resolution of 70 000 (FWHM) followed by a data-dependent MS/MS fragmentation of the top10 precursor ions (resolution 17 500; 1+ charge state excluded, isolation window of 1.6 *m/z*, normalized collision energy of 27%). The maximum ion injection time for MS scans has been set to 50 ms and for MS/MS scans to 120 ms. Protein identification was performed with Mascot software version 2.6.1 (Matrix Science Ltd., London, UK). Data were searched against SwissProt 2018_07/*E. coli* (23 042 sequences), a contaminant database (247 sequences) and an in-house database (402 sequences including entry of 6xHis-V5-3A). The following parameters were set: enzyme: trypsin/P with three missed cleavage, variable modifications: oxidation (M), trioxidation (C) and propionamide (C), mass tolerances for MS and MSMS: 5 p.p.m. and 0.02 Da. Proteins were accepted as identified if at least two unique peptides provided a Mascot MSMS score for identity ($P < 0.01$).

Statistics

Statistical analysis of the data was performed in GRAPHPAD PRISM v7.00 (GraphPad Software, San Diego, CA, USA). Data summary is depicted as mean \pm standard error of the mean. Unpaired *t*-test was used for two-group comparisons. If samples had unequal variances (determined by an *F* test), an unpaired *t*-test with the Welch correction was used. If values were normalized to internal control, one-sample *t*-tests were applied. For multiple group comparison, unequal variance versions of analysis of variance (one-way or two-way ANOVA) were performed followed by Sidak's or Tukey's multiple comparison test. The significance threshold

for all tests was set at the 0.05 level. To quantitatively compare the immunofluorescence frequency distributions and auto-correlation curve of the two genotypes, differences between single bins from wt protein 3A and 3A[C38A] were tested with a one-sample *t*-test against zero. We used a significance level of 0.05 and Bonferroni correction to correct for multiple testing of several bins.

Acknowledgements

We acknowledge Karolin Voss, Anika Linder and Kathrin Textoris-Taube for excellent technical assistance. The AMBIO (Advanced Medical Bioimaging Core Facility) at the Charité supported this project with confocal microscopy. Anti-3A antibody was a generous gift from J. Lindsay Whitton (The Scripps Research Institute, USA). AB is supported by the Deutsche Forschungsgemeinschaft (DFG, German Research Foundation) – Project-ID INST 39/1216-1-CRC/TRR 167 (B16N), DFG – Project-ID INST 247/893-1 – CRC1292 (TP02), DFG Project-ID BE 6335/4-3, CRC1470 (A08) and by the Foundation for Experimental Biomedicine Zurich, Switzerland. CB is supported by the International Max Planck Research School for Infection Biology. PS is supported by the Deutsche Forschungsgemeinschaft (DFG) through DFG - Project-ID 221545957, SFB 1078 (B06); DFG -Project-ID 421152132, CRC 1423 (A01/A05/Z03); DFG - Project-ID 394046635, CRC 1365 (A03); through Germany's Excellence Strategies – EXC2008/1 (UniSys-Cat) – 390540038 and through the Einstein Center of Catalysis (EC²). JS is supported by Deutsche Forschungsgemeinschaft (DFG) through SFB958 (Z02). Open access funding enabled and organized by ProjektDEAL.

Conflict of interest

The authors declare no conflict of interest.

Author contributions

Conceptualization: MV; Supervision: AB; Methodology: MV, KJ, SP, NG, MK, FI, CB and GK; Data acquisition: MV, MK and FT; Data analysis: MV, PMK, AB, KJ, NG, FT, GK and PS; Data visualization: MV, NG and GK; Funding acquisition: AB, JS, FI and PS; Writing ± original draft: MV, GK, PS, AB and P-MK.

Peer review

The peer review history for this article is available at <https://publons.com/publon/10.1111/febs.16368>.

Data availability statement

The data that supports the findings of this study are available in Figs 1–5 of this article and original files are available from the corresponding author [antje.beling@charite.de] upon reasonable request.

References

- Whitton JL, Cornell CT, Feuer R. Host and virus determinants of picornavirus pathogenesis and tropism. *Nat Rev Microbiol.* 2005;**3**:765–76.
- Thibaut HJ, De Palma AM, Neyts J. Combating enterovirus replication: state-of-the-art on antiviral research. *Biochem Pharmacol.* 2012;**83**:185–92.
- Baggen J, Thibaut HJ, Strating J, van Kuppeveld FJM. The life cycle of non-polio enteroviruses and how to target it. *Nat Rev Microbiol.* 2018;**16**:368–81.
- Voss M, Braun V, Bredow C, Kloetzel P-M, Beling A. Coxsackievirus B3 exploits the ubiquitin-proteasome system to facilitate viral replication. *Viruses.* 2021;**13**:1360.
- Wessels E, Notebaart RA, Duijsings D, Lanke K, Vergeer B, Melchers WJ, et al. Structure-function analysis of the coxsackievirus protein 3A: identification of residues important for dimerization, viral rna replication, and transport inhibition. *J Biol Chem.* 2006;**281**:28232–43.
- Klima M, Chalupska D, Rozycki B, Humpolickova J, Rezabkova L, Silhan J, et al. Kobuviral non-structural 3A proteins act as molecular harnesses to hijack the host ACBD3 protein. *Structure.* 2017;**25**:219–30.
- Horova V, Lyoo H, Rózycki B, Chalupska D, Smola M, Humpolickova J, et al. Convergent evolution in the mechanisms of ACBD3 recruitment to picornavirus replication sites. *PLoS Pathog.* 2019;**15**:e1007962.
- Smola M, Horova V, Boura E, Klima M. Structural basis for hijacking of the host ACBD3 protein by bovine and porcine enteroviruses and kobuviruses. *Arch Virol.* 2020;**165**:355–66.
- Cornell CT, Kiosses WB, Harkins S, Whitton JL. Inhibition of protein trafficking by coxsackievirus B3: multiple viral proteins target a single organelle. *J Virol.* 2006;**80**:6637–47.
- Strauss DM, Glustrom LW, Wuttke DS. Towards an understanding of the poliovirus replication complex: the solution structure of the soluble domain of the poliovirus 3A protein. *J Mol Biol.* 2003;**330**:225–34.
- Berman HM, Battistuz T, Bhat TN, Bluhm WF, Bourne PE, Burkhardt K, et al. The protein data bank. *Acta Crystallogr D Biol Crystallogr.* 2002;**58**:899–907.
- Schneider CA, Rasband WS, Eliceiri KW. NIH Image to ImageJ: 25 years of image analysis. *Nat Methods.* 2012;**9**:671–675.